SLAC-PUB-12124
August 2006

Coherent X-ray Production by Cascading Stages of High Gain Harmonic Generation Free Electron Lasers Seeded by IR Laser Driven High-Order Harmonic Generation*

Juhao Wu† and Paul R. Bolton
Stanford Linear Accelerator Center, Menlo Park, CA 94025

Coherent x-ray production achieved by a seeded free electron laser (FEL) with cascaded high gain harmonic generation (HGHG) is important for next generation development of synchrotron light sources. We examine the feasibility and some features of FEL emission seeded by a high order harmonic of an intense infrared conventional laser source (HHG). In addition to the intrinsic FEL chirp phenomenon, the longitudinal profile and spectral bandwidth of the HHG seed are modified significantly by the FEL interaction well before saturation occurs. This smears out original attosecond pulselet structure. As an example, we describe a cascaded HGHG scheme for coherent x-ray FEL generation that is seeded by the twenty-seventh harmonic of an ultrashort 800 nm laser pulse with 10 fs rms duration. By cascading two stages of HGHG, 15 GW peak power FEL emission at 0.3 nm can be produced with 90 MW peak power radiation at 0.1 nm via the non-linear harmonic generation.

Contributed to the 28th International Free Electron Laser Conference (FEL 2006), 8/27/2006-9/01/2006, Berlin, Germany

I. INTRODUCTION

Short-wavelength Free-electron Lasers (FELs) are perceived as the next generation synchrotron light sources. Self-Amplified Spontaneous Emission (SASE) [1–4], is the dominating approach to produce an x-ray FEL (XFEL). While it has good transverse coherence, the SASE FEL pulses are composed of a series of ultrashort spikes due to a short longitudinal coherent length. To improve the longitudinal coherence, various approaches have been proposed. Among them, a cascaded high gain harmonic generation (HGHG) FEL [5–10] looks promising by invoking high order harmonic generation of an infrared (ir) laser (HHG) as the seed. In this paper, we study an HHG seeded FEL. This is of particular interest [11], since HHG can provide a uv to soft x-ray seed, making a coherent hard XFEL feasible.

II. HHG SEEDED HGHG FELS AT LCLS

A. HHG Seed: Attosecond Structure and Smearing Effect

HHG generates an electric field comprised of multiple harmonic orders, s and multiple time pulselets, n expressed as the following double summation [12, 13]:

$$E_{\rm HHG}(t,z) = \sum_s E_{s,0} e^{i(k_s z-\omega_s t)} e^{-i\mathcal{B}_s\omega_s^2 t^2} \times \sum_{n=-N}^{N} e^{-\frac{t_n^2}{4\sigma_{t,0}^2}} e^{-\alpha_s\omega_s^2[(t-t_n)-z/c]^2}, \quad (1)$$

where for each order, s we sum over the temporal sequence of $2N+1$ pulselets for which $n \in [-N, N]$. Because of temporal coherence of a group of harmonic orders, the pulselets can exhibit attosecond structure (with periodicity of $\tau/2$), limited by the relative amplitudes and phases of the different harmonic orders. The order dependent parameter, $\mathcal{B}_s$ accounts for the small intrinsic chirp that characterizes each harmonic order [14]. In Eq. (1), $t_n = n\tau/2$ with τ being the period of the unchirped ir pulse (2.67 fs at 800 nm); $\sigma_{t,0}$ is the ir pulse rms duration; k_s and ω_s are the wavenumber and angular frequency of the s^{th} harmonic; and $\alpha_s = (4\sigma_{t,s}^2\omega_s^2)^{-1}$ with $\sigma_{t,s}$ being the rms duration of each pulselet in the HHG pulse. Typically $\sigma_{t,0} \approx 10$ fs and $\tau/20 \le \sigma_{t,s} \le \tau/2$ for a single pulselet, where the lower limit assumes relative phase synchronization of a harmonics group [12, 15]. In this paper, we consider only a single harmonic order, s as the carrier frequency and for simplicity, we negelect the harmonic chirp ($\mathcal{B}_s \approx 0$). The HHG field expression then simplifies to:

$$E(t,z) = E_{s,0} e^{i(k_s z-\omega_s t)} \sum_{n=-N}^{N} e^{-\frac{t_n^2}{4\sigma_{t,0}^2}} \times e^{-\alpha_s\omega_s^2[(t-t_n)-z/c]^2}, \quad (2)$$

which represents an attosecond pulselet train (APT) derived from the amplitude modulation of carrier frequency, ω_s. We use $\sigma_{t,0} = 10$ fs and $\sigma_{t,s} = \tau/8 \approx 334$ attosecond in the Fourier-transform limit. In this case, it is important to note that, although the central carrier frequency of the seed is a single harmonic, the transform limited seed spectrum also includes components from several neighboring harmonic orders [16]. A multi-pulselet HHG seed is the sum of many single pulselets. We address the single pulselet at $t_n = 0$ for $n = 0$ so that $E_s(t, z=0) = E_{s,0}\exp(-i\omega_s t - \alpha_s\omega_s^2 t^2)$, assuming for simplicity that the single harmonic pulselet is transform-limited, *i. e.*, $\sigma_{t,s}\sigma_{\omega,s} = 1/2$, so that the rms bandwidth

*The work was supported by the US Department of Energy under contract DE-AC02-76SF00515.
†Electronic address: jhwu@SLAC.Stanford.EDU

$\sigma_{\omega,s} = \sqrt{\alpha_s}\omega_s$. Since each pulselet is ultra short, the spectral bandwidth is broad. The seeded FEL solution reads [17, 18]

$$E_{\rm FEL}(t,z) = E_{0,\rm FEL}e^{\rho(\sqrt{3}+i)k_w z} \times e^{i(k_s z-\omega_s t)}e^{-[\alpha_{s,f}(z)+i\beta_{s,f}(z)]\omega_s^2(t-z/v_g)^2}, \quad (3)$$

where $v_g = \omega_s/(k_s + 2/3k_w)$ is the group velocity of the FEL light,

$$\alpha_{s,f}(z) = \frac{1}{4\sigma_{t,s,f}^2(z)\omega_s^2}, \quad (4)$$

and

$$\beta_{s,f}(z)^2 = \alpha_{s,f}(z)\frac{\sigma_{\omega,s,f}^2(z)}{\omega_s^2} - \alpha_{s,f}(z)^2 \quad (5)$$

with

$$\begin{cases} \sigma_{t,s,f}(z) = \sigma_{t,s}\sqrt{\frac{3+6R(z)^2+4R(z)^4}{3[1+R(z)^2]}} \\ \sigma_{\omega,s,f}(z) = \frac{\sigma_{\omega,s}}{\sqrt{1+R(z)^2}} \end{cases}, \quad (6)$$

with

$$R(z) \equiv \frac{\sigma_{\omega,s}}{\sigma_{\omega,\rm GF}(z)}, \quad (7)$$

and

$$\sigma_{\omega,\rm GF}(z) \equiv \sqrt{\frac{3\sqrt{3}\rho\omega_s^2}{k_w z}}. \quad (8)$$

Here $\sigma_{\omega,\rm GF}(z)$ is the rms bandwidth of the FEL Green function for a coasting electron beam with ρ being the Pierce parameter [1]. The transform limit also means that $\alpha_{s,f}(0) = \alpha_s$, $\beta_{s,f}(0) = \beta_s = 0$, $\sigma_{t,s,f}(0) = \sigma_{t,s}$, and $\sigma_{\omega,s,f}(0) = \sigma_{\omega,s}$. The FEL-interaction intrinsically generates a chirped FEL waveform,

$$\langle(t-\langle t\rangle)(\omega-\langle\omega\rangle)\rangle = \frac{\beta_{s,f}(z)}{2\alpha_{s,f}(z)} = \frac{R(z)^2}{2\sqrt{3}[1+R(z)^2]}. \quad (9)$$

The emittance of the FEL light at any position, z, is conserved, $\varepsilon \equiv \{\langle(t-\langle t\rangle)^2\rangle\langle(\omega-\langle\omega\rangle)^2\rangle - \langle(t-\langle t\rangle)(\omega-\langle\omega\rangle)\rangle^2\}^{1/2} = 1/2$, indicating that the FEL emission is fully coherent longitudinally [17].

We introduce the critical location, z_c, where the FEL Green function bandwidth reduces to the pulselet initial bandwidth, *i.e.*, $R(z_c) = 1$. Recall that, the power gain length $L_{\rm G} = \lambda_w/(4\sqrt{3}\pi\rho)$, hence, if $\sigma_{\omega,s}/\omega_s > 3\sqrt{2}\rho$, then $z_c < L_{\rm G}$. For large enough z, where $R(z) \gg 1$, the FEL has

$$\begin{cases} \sigma_{t,s,f}(z) \to \frac{1}{\sqrt{3}\sigma_{\omega,\rm GF}(z)} \\ \sigma_{\omega,s,f}(z) \to \sigma_{\omega,\rm GF}(z) \\ \langle(t-\langle t\rangle)(\omega-\langle\omega\rangle)\rangle \to \frac{1}{2\sqrt{3}} \end{cases}, \quad (10)$$

i.e., the final characteristics are determined by the FEL interaction. In accordance with Eq. (6), the FEL interaction rapidly reduces the seed pulselet bandwidth, extending its duration [16].

B. HHG-HGHG FELs at LCLS

Considering the feasibility of an HHG seeded HGHG XFEL, we use an ir laser at 800 nm with $\sigma_{t,0} = 10$ fs. We choose the 27^{th} harmonic as the seed to interact with an LCLS-type high brightness electron bunch [19]. The initial pulselet is assumed to have $\sigma_{t,s} = \tau/8$. Assuming a Fourier-transform limited single harmonic pulselet, we have $\sigma_{\omega,s} = 1/(2\sigma_{t,s})$. The relative rms bandwidth is $\sigma_{\omega,s}/\omega_s \approx 2.4$ %. Due to the FEL interaction, according to Eq. (7), the FEL bandwidth decreases. For the scheme shown in Fig. 1 with parameters in Table I, we have $\rho = 0.54$ % and $\lambda_w = 0.2$ m, we have $z_c \approx 1.6$ m. Considering that the first modulator is 25 m long and the power gain length is about 3 m, attosecond structure is smeared out within a short distance [16]. Consequently, the HHG seed resembles a conventional harmonic seed generated via wave-mixing in a solid such that we can ignore initial attosecond structure, at least as a good approximation.

In Fig. 1, we show the generic configuration of an HHG seeded cascaded HGHG FEL. It has the following features.

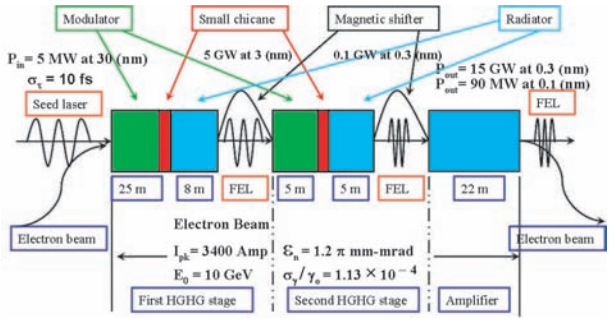

FIG. 1: Schematics of an HHG seeded cascaded HGHG FEL. In this scheme an HHG seed of 30 nm is used. After two stages of HGHG and a final amplifier, we obtain 15 GW at 0.3 nm, and 90 MW at 0.1 nm.

1. We need multiple stages. During each stage the nth harmonic of the seed laser will be produced at the end of the radiator, and then this harmonic will be used as the seed for the next stage. In reality, n cannot be too large due to that stability consideration [7, 9]. In our paper we use $n = 10$ to achieve stable performance, and we need only two stages.

2. Conceptually, the device is composed of two parts: a converter [20] and an amplifier. The converter, consisting of several stages, converts the seed laser to the designed wavelength step by step. Then at the end, an amplifier exponentially amplifies the radiation obtained from the last stage to saturation.

3. Except for the first modulator and the last amplifier, each stage only converts the light to its n^{th} harmonic. Exponential growth is not required as long as the harmonic power is high enough to be used as the seed for the next stage.

4. The phase mixing induced by the emittance in the

dispersion section is much smaller than that in an undulator. For an HGHG FEL, bunching is produced mainly in the dispersion section; while for a SASE FEL, bunching is produced in the undulator. Therefore, the emittance effect turns out to be less important in an HGHG FEL than in a SASE FEL [10].

5. Since we need to cascade several stages of HGHG, we need some extra components. Each stage will consist of one modulator, a dispersion section (a small chicane), and one radiator. The physics process in each stage will be the same as in Refs. [5, 6]. During the process, the output radiation has disturbed the coincident part of the e-bunch. Therefore, to achieve the best efficiency in the next stage of HGHG, we need use a fresh region of the e-bunch. To do this, the laser (i.e., the output radiation from the previous HGHG stage) is shifted to the front part of the same e-bunch, so that the laser will interact with a fresh part of the same e-bunch. *i.e.*, we use a magnetic shifter to relatively delay the electron bunch.

As mentioned above, this conceptual design uses the 27^{th} harmonic of the 800 nm ir pulse with $\sigma_{t,0} = 10$ fs. Assuming the input seed peak power of 5 MW, with two stages of HGHG and a final amplifier, we obtain a 15 GW FEL at 0.3 nm, and 90 MW at 0.1 nm via nonlinear harmonic generation [21, 22]. In this example, the 27^{th} harmonic pulselet interacts with an LCLS-type electron beam [19] (normalized emittance $\varepsilon_n = 1.2$ π mm-mrad, relative energy spread $\sigma_\gamma/\gamma_0 = 1.13\times10^{-4}$, energy $E_0 = 10$ GeV, and peak current $I_{pk} = 3,400$ Amp). In the 25 m modulator of the first HGHG stage, the HHG seed is amplified, and simultaneously modulates the electron beam energy. A small chicane then converts the energy modulation into density microbunching at 30 nm. This microbunched electron beam then traverses the 8 m radiator which is resonant at 3 nm (the 10^{th} harmonic of the original 30 nm seed). This microbunched electron beam first coherently radiates at 3 nm and then exponentially amplifies this 3 nm radiation to a peak power of 5 GW, which is used to seed the next HGHG stage. In the second stage, the 5 GW, 3 nm seed energy modulates the electron beam in the 5 m modulator. The energy modulation is converted into density microbunching at 3 nm via a second small chicane. This density modulated electron beam initially radiates coherently in the 5 m radiator, resonant at 0.3 nm (the 10^{th} harmonic of the 3 nm seed). At the end of the 5 m radiator, the 0.3 nm radiation is amplified to 0.1 GW, which is further amplified in the 22 m final amplifier, resonant at 0.3 nm. At the amplifier exit, the FEL is well into saturation, and the system finally produces 15 GW, 0.3 nm radiation. Due to the microbunching at 0.3 nm, there are substantial harmonics. The third harmonic emission at 0.1 nm has a peak power of 90 MW.

As shown in Fig. 1, we consider an HHG seed with a wavelength of 30 nm, and a peak power of $P_{\rm in} = 5$ MW. As we will discuss later, the corresponding start-up shot-noise power is only about $P_{\rm noise} \approx 30$ W. Thus the input seed laser power dominates the shot-noise power.

	1^{st} stage		2^{nd} stage		Amplifier
λ_r (nm)	30	3	3	0.3	0.3
λ_w (cm)	20	6	6	3	3
$\frac{d\psi}{d\gamma}$	0.2		0.4		
$\frac{\sigma_\gamma}{\gamma_0}$	1.13×10^{-4}				
L_w (m)	25	8	5	5	22
L_G (m)	3	2	2	3	3

TABLE I: Parameters for the undulator, the dispersive section and the electron bunch.

This dominance is necessary, because even though there is only negligible noise power in the initial stage, the signal-to-noise ratio of the final radiation at 0.3 nm can be degraded [23]. A simple estimate shows that the noise-to-signal (NTS) ratio at the seed will be amplified by $n_{\rm tot}^2$ times for the $n_{\rm tot}^{th}$ harmonic generation. In this case, the two stage approach has an overall $n_{\rm tot} = 100$, hence, the NTS ratio will be amplified by 10^4 times. Hence for the final radiation at 0.3 nm, the NTS ratio will be about 6 %.

After two HGHG stages, we have generated 0.3 nm radiation, and this 0.3 nm radiation is amplified to saturation with a peak power near 15 GW in a final amplifier stage. The parameters for the electron beam and the radiation are given in Fig. 1. The number in the first row stands for the output power and wavelength of the radiation of each stage. The output power of one stage is the input power of the next stage, though diffraction has been taken into consideration in the simulation. The e-beam parameters are printed below the schematic device. The relative local energy spread σ_γ/γ_0 given in Fig. 1 is the initial relative local energy spread before the e-beam enters the first modulator. This is increased by spontaneous radiation [24]. We take this into account in the simulation [22].

In Table I, the first row gives the radiation wavelength λ_r; the second row, the undulator period λ_w, and the third row the dispersion strength $d\psi/(d\gamma)$ with ψ being the ponderomotive phase in the radiator. The fourth row gives the initial relative local energy spread σ_γ/γ_0. In our simulation, quantum diffusion [24] has been taken into account [22]. The fifth row gives the length of the undulators (modulators, radiators, and the amplifier) L_w. For example, the last amplifier has a length of 22 m. The sixth row gives the power gain length L_G in each undulator without energy modulation. The table has three boxes; the first two boxes are for the two convertor stages and the last one is for the amplifier. For the two convertor stages, the left column gives the parameters for the modulator and the right column those for the radiator; the numbers in the middle stand for the dispersion strength $d\psi/(d\gamma)$. For example, the left column in the second box stands for the modulator of the second stage. The table shows that in the modulator the resonant radiation has a wavelength of 3 nm, the modulator has a period of 6 cm, the length of the modulator is 5 m, and

the corresponding power e-folding length without energy modulation is 2 m. The right column shows that the radiation in the radiator has a wavelength of 0.3 nm, the radiator has a period of 3 cm, the length of the radiator is 5 m, and the corresponding power e-folding length is 3 m. In the middle, i.e. 0.4, stands for the dispersion strength $d\psi/(d\gamma)$.

C. Start-up Noise Issue

First, we need to compute the effective start-up noise power for the fundamental SASE guiding mode [9, 25]

$$P_{\rm SASE}^{\rm Start-up} = C_1 \frac{2L_G}{L_w}\pi\left(\frac{2\lambda_r}{L_w}\right)\sqrt{\frac{3\sqrt{3}\rho}{N_w}} \times \frac{eZ_0 I_{pk}}{4\pi}N_w^2\gamma^2\frac{K^2}{\left(1+\frac{K^2}{2}\right)^2}[JJ]^2\omega_r, \quad (11)$$

where the coupling factor is found to be [25],

$$C_m(a) \approx \frac{\sqrt{3}}{\pi a^2}\exp\left[-\frac{1}{a\sqrt{1+a^2}}\left(\beta_{m,0}+\beta_{m,1}\frac{1}{a^2}\right)\right], \quad (12)$$

where, m is the index referring to a certain mode being excited; $a = \sqrt{4\rho k_w k_r}R_0$ is the scaled beam size with $k_w = 2\pi/\lambda_w$, $k_r = 2\pi/\lambda_r$, and R_0 the hard edge of an electron beam. The above formula is a good approximation, when $a > 0.25$. Within such range, $\beta_{m,0} = 1.093$, and $\beta_{m,1} = -0.02$ for the fundamental guiding mode. In Eq. (11), L_G is the power gain length; L_w the undulator length; λ_r the radiation wavelength; N_w the number of undulator period; Z_0 the vacuum impedance; I_{pk} the peak current; $\omega_r(= c2\pi/\lambda_r)$ the radiation angular frequency with c the speed of light in vacuum. The Bessel factor $[JJ] = J_0\left[\frac{a_w^2}{2(1+a_w^2)}\right] - J_1\left[\frac{a_w^2}{2(1+a_w^2)}\right]$, with $a_w = K/\sqrt{2}$, and J_0 and J_1 are the zeroth order and first order Bessel function, respectively. Approximately, $K \approx 93.4 B_w\lambda_w$ is the undulator parameter with B_w the peak field of the undulator in units of Tesla and λ_w in units of meter.

In the above SASE calculation, the bandwidth of the fundamental guided mode is $\sigma_{\omega,\rm GF}$ for $z = 2L_G$ according to Eq. (8). However, the seeded FEL has a different bandwidth of $\sigma_{\omega,s,f}(z = 2L_G)$ according to Eq. (6). Hence, the true start-up noise power in the seeded FEL bandwidth is

$$P_{\rm Seeded}^{\rm Start-up} = P_{\rm SASE}^{\rm Start-up}\frac{\sigma_{\omega,s,f}(z=2L_G)}{\sigma_{\omega,\rm GF}(z=2L_G)}. \quad (13)$$

Considering the first modulator, the Pierce parameter is $\rho \approx 5.4\times10^{-3}$; the scaled beam size is $a \approx 0.8$, which gives the coupling coefficient to be $C_1 \approx 0.3$. According to Eq. (11), the SASE effective start-up noise power in the fundamental guided mode is $P_{\rm SASE}^{\rm Start-up} \approx 400$ W. However, the seeded FEL has a different bandwidth compared to the SASE FEL; hence, we need compute the start-up noise power in the seeded FEL bandwidth. As we show in Sec. II B, $z_c \approx 1.6$ m $\ll 2L_G(= 6$ m), the attosecond structure is smeared out [16]; hence, the relevant bandwidth is due to the entire harmonic pulse train. In our design, we assume the initial HHG seed rms pulse length is $\sigma_{t,0} = 10$ fs. Further assuming a transform limited pulse, the initial seed spectral rms bandwidth is $\sigma_{\omega,s} = 1/(2\sigma_{t,0})$. The start-up noise power is evaluated at location $z = 2L_G$ as in Eq. (11) [9, 25], therefore, we need compare the bandwidth of the SASE FEL with that of the seeded FEL at location $z = 2L_G$. According to Eq. (6), at $z = 2L_G$, the seeded FEL bandwidth is $\sigma_{\omega,s,f}(z = 2L_G)/\omega_s \approx 0.8\times10^{-3}$. At the same location, $z = 2L_G$, according to Eq. (8), the SASE bandwidth is $\sigma_{\omega,\rm GF}(z = 2L_G)/\omega_s \approx 1.2$ %. Consequently, the true start-up noise power in the seeded FEL bandwidth is only about $P_{\rm Seeded}^{\rm Start-up} \approx 30$ W.

III. DISCUSSION

In this paper, we explored the details of an HHG seeded FEL. For simplicity, the HHG seed is modelled as an attosecond pulselet train (APT). Bandwidth reduction, intrinsic to the FEL interaction, smears out the initial attosecond structure of the seed within a very short distance, $z < L_G$. The seeded FEL remains coherent, if we do not consider the accompanied noise power and electron beam non-uniformity [10]. The true start-up noise power in the seeded FEL bandwidth, $P_{\rm Seeded}^{\rm Start-up}$ is only about 30 W. Since the HHG seed has a power of $P_{\rm in} = 5$ MW, the noise-to-signal ratio at the final radiation $\lambda_r = 0.3$ nm is still only about 6 %, even though it has $n_{\rm tot}^2 = 10^4$ ($n_{\rm tot} = 100$) times amplification, *i.e.*, the effective noise level is increased from the initial 30 W to 0.3 MW.

[1] R. Bonifacio, C. Pellegrini, L.M. Narducci, Opt. Commun., **50**, 373 (1984).

[2] J.-M. Wang and L.-H. Yu, Nucl. Instr. and Meth., **A 250**, 484 (1986).

[3] K.-J. Kim, Nucl. Instr. and Meth., **A 250**, 396 (1986); Phys. Rev. Lett. **57**, 1871 (1986); Lawrence Berkeley National Loboratory Report No. 40672 (1997).

[4] S. Krinsky and Z. Huang, Phys. Rev. ST Accel. Beams **6**, 050702 (2003); E.L. Saldin *et al.*, *Proc., 2005 Int. FEL Conf.*, p.258.

[5] L.H. Yu, *Phys. Rev. A* **44**, 5178(1991).

[6] L.-H. Yu, *et al.*, *Science*, **289**, 932(2000).

[7] J. Wu and L.H. Yu, Nucl. Instr. and Meth., **A 475**, 104 (2001);

[8] L.H. Yu and J. Wu, Nucl. Instr. and Meth., **A 483**, 493 (2002).
[9] J. Wu and L.H. Yu, Stanford Linear Acclerator Center Report No. SLAC-PUB-10494 (2004).
[10] J. Wu and L.H. Yu, Stanford Linear Acclerator Center Report No. SLAC-PUB-10495 (2004).
[11] M.-E. Couprie *et al.*, *Proc., 2005 Int. FEL Conf.*, p.55.
[12] R. López-Martens, Phys. Rev. Lett. **94**, 033001 (2005).
[13] E.A. Gibson *et al.*, IEEE J. of Selected Topics in Quant. Elec. **10**, 1339 (2004).
[14] J. Mauritsson *et al.*, Phys. Rev. A **70**, 021801(R) (2004).
[15] P.M. Paul *et al.*, Science **292**, 1689 (2001).
[16] J. Wu, P.R. Bolton, J.B. Murphy, and X. Zhong, Stanford Linear Acclerator Center Report No. SLAC-PUB-11891 (2006).
[17] J.B. Murphy *et al.*, Brookhaven National Laboratory Report No. BNL-75807-2006-JA, and Stanford Linear Acclerator Center Report No. SLAC-PUB-11852 (2006).
[18] J. Wu *et al.*, Stanford Linear Acclerator Center Report No. SLAC-PUB-11985 (2006).
[19] J. Arthur *et al.*, Stanford Linear Acclerator Center Report No. SLAC-R-593 (2002).
[20] I. Boscolo and V. Stagno, *Nuovo Cimento B* **56**, 219(1980).
[21] Z. Huang and K.J. Kim, Phys. Rev. E **62**, 7295 (2000).
[22] J. Wu, *Proc., 2003 Particle Accel. Conf.*, p. 1035.
[23] E.L. Saldin, E.A. Schneidmiller, and M.V. Yurkov, *Opt. commun.* **202**, 169 (2002).
[24] E.L. Saldin, E.A. Schneidmiller, and M.V. Yurkov, *Nucl. Instrum. Methods Phys. Res. A* **381**, 545(1996)
[25] L.H. Yu, *Phys. Rev. E* **58**, 4991(1998).